

Static analysis of thin-walled beams using two-phase local-nonlocal integral model

M. G. GÜNAY

*Isparta Applied Sciences University, Technology Faculty,
Mechanical Engineering Department, Isparta, Turkey,
e-mail: muhsingunay@isparta.edu.tr*

A MATHEMATICAL MODEL IS DEVELOPED FOR STATIC ANALYSIS of small-scale thin-walled beams having arbitrary cross sections. Constitutive relations of the thin-walled beams are defined upon the two-phase local-nonlocal mixture model with integral formulation. The developed model includes flexural-torsional coupling and warping effects. Governing equations of the thin-walled beams having nonlocal property are derived by using the principle of minimum potential energy. The displacement based finite element method is used to solve both local and nonlocal part of the model. The effect of the nonlocal parameters on the static behavior of micro-scale thin-walled beams having closed and open cross-sections is examined and discussed for various nonlocal parameters and boundary conditions.

Key words: static analysis, nonlocal elasticity, two-phase, thin-walled, small-scale beams.



Copyright © 2023 The Author.

Published by IPPT PAN. This is an open access article under the Creative Commons Attribution License CC BY 4.0 (<https://creativecommons.org/licenses/by/4.0/>).

1. Introduction

THIN-WALLED BEAMS MAY OCCUR NATURALLY or they can be prepared artificially. Natural or artificial thin-walled beams appear in many fields of our modern life from the nano to the macro scale. Compared to solid beams with the same cross-sectional area, thin-walled beams have greater flexural rigidity. This makes them preferred structural elements in many applications. The usage of thin-walled beams as structural elements dates back to ancient civilizations. Nowadays, the use of thin-walled beams in steel frames and light weight structures has increased the interest in them. Hereby engineering calculations on thin-walled beams get more sophisticated. In this manner studies of TIMOSHENKO and GOODIER [1] can be counted as one of the first modern studies on thin-walled beams. Works of VLASOV [2] and GJELSVIK [3] set the standards on the modelling of thin-walled beams. While metal thin-walled beams are usually used in buildings and chassis of vehicles, thin-walled beams made of composite materials usually are preferred at lightweight structures. LIBRESCU and SONG [4]

compiled previous studies on the topic and developed a theory for thin-walled composite beams.

As the dimensions of a structure reduces from macro to micro/nano scale inhomogeneous properties such as atomic structure, grain size and orientation, material voids etc. may get effective on the mechanical behavior of the structure. In this case classical continuum equations can be enriched by using theories such as nonlocal elasticity [5], strain gradient [6], micropolar [7] and surface elasticity [8] to account for this kind of small-scale effects.

Nonlocal beams modelled by the Euler–Bernoulli beam theory and Eringen’s nonlocal elasticity theory has been specifically addressed in the literature. It has been indicated that these nonlocal models show ill-posed properties [9–12] for some boundary conditions, especially for cantilever beams under a concentrated tip load. But, when the studies indicating this problem are examined, it is seen that the mentioned ill-posed case occurs when the constitutive relations are expressed by using the strain driven differential form [9] instead of the original integral form [5] of the nonlocal elasticity theory. To overcome this situation several models and solutions are developed in the literature such as the gradient elasticity model [10, 13], local-nonlocal mixture model [10, 14], lattice based model [15], stress driven model [16–19] and enhanced models [20]. Additional to these models, CHALLAMEL *et al.* [21] managed to solve the cantilever beam problem by applying a discontinuous rotation field at the acting point of the concentrated load. They also solved the mentioned cantilever beam problem by modelling the cantilever beam as half of a simply supported beam and acquired the same results with the discontinuous rotation field solution. Latterly, FERNANDEZ *et al.* [22] compared the differential formulation and the integral formulation of the nonlocal elasticity theory for nonlocal beams. And they mentioned that while converting the integral formulation to the differential formulation, the conditions described by POLYANIN and MANZHIROV [23] must be fulfilled. They stated that if these conditions are not fulfilled the differential formulation may lead to abnormal trends [22]. Additionally, FERNANDEZ *et al.* [22] showed that the integral formulation can be used for any boundary condition and loading case.

Even though the small-scale effect theories are mostly used for investigation of nano structures, the usage of these theories on micro-scale structures has been increasing recently. LI *et al.* [24] examined vibrational behavior of microbeams having circular and rectangular cross-sections based on the modified couple stress theory. But still there are a few studies which combine thin-walled beam theories with small-scale effect theories in the literature. GHANE *et al.* [25] investigated vibrations of fluid-conveying thin-walled nanotubes by using the nonlocal strain gradient theory. SOLTANI *et al.* [26] used the differential form of Eringen’s nonlocal theory to analyze the stability of small-scale tapered I-beams with axially varying material properties.

Recently, GÜNAY has investigated buckling [27] and vibration [28] of nano/micro scale nonlocal thin-walled beams. Unlike the author’s previous works this study focuses on the static analysis of nonlocal thin-walled beams, including the problem of a nonlocal cantilever beam under a concentrated tip load. Results of the developed model are compared with the results and solutions available in the literature. It is validated that the developed model is capable of performing static analysis of small-scale thin-walled beams showing a nonlocal property for any loading or boundary condition. This is achieved by defining the constitutive relations of the thin-walled beams theory [4] with two phase local-nonlocal integral formulation [5, 14]. As numerical examples, effects of the nonlocal parameters on the deformation of the micro-scale thin-walled beams are investigated and discussed for several boundary and loading conditions.

2. Kinematics

Thin-walled beams theory developed by VLASOV [2] and latterly by LIBRESCU [4] depends on the idea of reducing three-dimensional geometry of the thin-walled beam to an elastic line which is called as the pole. The intersection of the cross-section plane and the pole called as the pole point $P(x_p, y_p)$ which moves with the cross-section. By assuming that the cross section of the beam does not change its shape in its own plane during deformation, the U, V displacements and ϕ rotation of the cross section can be defined depending on the pole point. Two coordinate systems are used in formulations as seen in Fig. 1. The first one is the global (x, y, z) Cartesian coordinate system and the second one is the local (s, n, z) coordinate system placed on the middle surface.

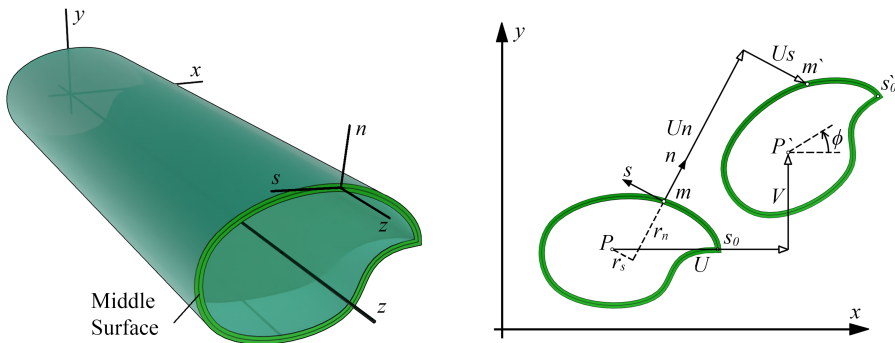


FIG. 1. Coordinate systems and displacements of an arbitrary point (m) on the middle surface.

By neglecting the transverse shear stresses and allowing the cross-section to warp perpendicular to its own plane, displacements of an arbitrary point-A

which is (n) units away from the middle surface can be expressed in terms of U and V displacements and ϕ rotation as given below [4]:

$$(2.1a) \quad U_s(s, z, n) = U(z) \frac{dx}{ds} + V(z) \frac{dy}{ds} + \phi(z)(r_n(s) + n),$$

$$(2.1b) \quad U_n(s, z) = U(z) \frac{dy}{ds} - V(z) \frac{dx}{ds} - \phi(z)r_s(s),$$

$$(2.1c) \quad W(s, z, n) = W_0(z) - U'(z) \left(x(s) + n \frac{dy}{ds} \right) - V'(z) \left(y(s) - n \frac{dx}{ds} \right) \\ - \phi'(z)(\mathcal{F}_1(s) + n\mathcal{F}_2(s)),$$

where W_0 is the axial displacement of the origin of the cross-section contour (s_0), $r_n(s)$ is the distance to the pole point in normal direction and similarly $r_s(s)$ is the distance to the pole point in the tangential direction. $\mathcal{F}_1(s)$ and $\mathcal{F}_2(s)$ are the primary and secondary warping functions which depend on the shape of the cross-section. Definitions of these terms are given in Appendix A.1. Based on the small deformation assumption, the ε_{ss} , ε_{nn} and γ_{sn} strains are neglected and the remaining ε_{zz} axial and γ_{sz} , γ_{nz} shear strains of the thin-walled beam are expressed as:

$$(2.2a) \quad \varepsilon_{zz} = \frac{dW}{dz} = \varepsilon_{zz}^{(0)} + n\varepsilon_{zz}^{(1)},$$

$$(2.2b) \quad \gamma_{sz} = \frac{\partial W}{\partial s} + \frac{\partial U_s}{\partial z} = \gamma_{sz}^{(0)} + n\gamma_{sz}^{(1)},$$

$$(2.2c) \quad \gamma_{nz} = \frac{\partial W}{\partial n} + \frac{\partial U_n}{\partial z} = 0,$$

where $(\dots)^{(0)}$ indicates the middle surface strains and $(\dots)^{(1)}$ indicates the middle surface curvatures.

3. Governing equations

Equilibrium equations of the thin-walled beam are obtained by equating the variation of the total potential energy of the system to zero. The total potential energy of the system is the sum of the strain energy and the work done by external forces and a moment

$$(3.1) \quad \Pi_{total} = \Pi_{strain} + \mathcal{W}_{ext},$$

where the strain energy is defined as:

$$(3.2) \quad \Pi_{strain} = \frac{1}{2} \int_v (\sigma_{zz}^{(k)} \varepsilon_{zz} + \sigma_{sz}^{(k)} \gamma_{sz}) dv.$$

By substituting Eqs. (2.2a) and (2.2b) into Eq. (3.2) and expanding the displacement terms the strain energy is obtained as given below

$$(3.3) \quad \Pi_{strain} = \frac{1}{2} \int_v \left\{ \sigma_{zz}(s) \left[W'_0 - U'' \left(x + n \frac{dy}{ds} \right) - V'' \left(y - n \frac{dx}{ds} \right) - \phi'' (\mathcal{F}_1(s) + n\mathcal{F}_2(s)) \right] + \sigma_{sz}(s) \left[\delta_c \frac{2\Omega}{h(s)G_{sz}(s)\mathcal{L}} + n \left(\delta_c \frac{2\beta}{h(s)G_{sz}(s)\mathcal{L}} + \delta_o 2 \right) \right] \phi' \right\} dv.$$

This equation can be rearranged by using stress resultants as:

$$(3.4) \quad \Pi_{strain} = \frac{1}{2} \int_0^l (N_z W'_0 - M_x V'' - M_y U'' + M_z \phi' - M_\omega \phi'') dz,$$

where $(N_z, M_x, M_y, M_\omega, M_z)$ are the beam forces and the moments which are defined below:

$$(3.5a) \quad N_z = \int_c \int_{-h/2}^{h/2} \sigma_{zz} dn ds,$$

$$(3.5b) \quad M_x = \int_c y \int_{-h/2}^{h/2} \sigma_{zz} dn + \int_{-h/2}^{h/2} n \sigma_{zz} dn \frac{dx}{ds} ds,$$

$$(3.5c) \quad M_y = \int_c x \int_{-h/2}^{h/2} \sigma_{zz} dn - \int_{-h/2}^{h/2} n \sigma_{zz} dn \frac{dy}{ds} ds,$$

$$(3.5d) \quad M_\omega = \int_c \int_{-h/2}^{h/2} \sigma_{zz} dn \mathcal{F}_1(s) - \int_{-h/2}^{h/2} n \sigma_{zz} dn \mathcal{F}_2(s) ds,$$

$$(3.5e) \quad M_z = \int_c \int_{-h/2}^{h/2} \sigma_{sz} dn \left(\delta_c \frac{2\Omega}{h(s)G_{sz}(s)\mathcal{L}} \right) - \int_{-h/2}^{h/2} n \sigma_{sz} dn \left(\delta_c \frac{2\beta}{h(s)G_{sz}(s)\mathcal{L}} + \delta_o 2 \right) ds.$$

The work done by external forces and moments is calculated as:

$$(3.6) \quad \mathcal{W}_{ext} = \int_0^l (q_z \cdot W_0 + q_x \cdot U + q_y \cdot V + m_z \cdot \phi) dz,$$

where q_x and q_y are distributed transverse loads, q_z is the distributed axial load and m_z is the distributed axial torque. By substituting Eq. (3.4) and Eq. (3.6) into Eq. (3.1) then equating the first variation of the total potential energy to zero, the following weak formulation is obtained:

$$(3.7) \quad \int_0^l (N_z \cdot \delta W'_0 - M_x \cdot \delta V'' - M_y \cdot \delta U'' + M_z \cdot \delta \phi' - M_\omega \cdot \delta \phi'' + q_z \delta W_0 + q_x \delta U + q_y \delta V + m_z \delta \phi) dz = 0.$$

4. Constitutive relations

As mentioned in the introduction section, some nonlocal beam models may show ill-posed properties for some loading cases, especially for cantilever beams. This situation can be avoided by using integral formulation as mentioned by FERNANDEZ *et al.* [22]. Considering this situation, constitutive relations of the developed model are defined by using the two-phase local-nonlocal mixture model with integral formulation. The two-phase local-nonlocal mixture model combines the classical local elasticity and nonlocal elasticity models. In general, constitutive relations of a structure can be expressed with the two-phase local-nonlocal mixture model as given below [5, 14]

$$(4.1) \quad t_{kl}(\vec{x}, t) = \xi_1 E_{ijkl} \varepsilon_{kl}(\vec{x}, t) + \xi_2 \int_V \alpha(|\vec{x} - \vec{x}'|, \tau) E_{ijkl} \varepsilon_{kl}(\vec{x}', t) dx',$$

$$(4.2a) \quad \vec{x} = \{x, y, z\},$$

$$(4.2b) \quad \vec{x}' = \{x', y', z'\},$$

where $\alpha(|\vec{x} - \vec{x}'|, \tau)$ is the non-local kernel function which defines the influence of the neighboring points (\vec{x}') to the actual point (\vec{x}), τ is the nonlocal parameter in length units, E_{ijkl} is the material constants and ε_{kl} is the strain component; ξ_1 and ξ_2 are volume fractions of classical local elasticity and nonlocal integral elasticity, respectively. By definition summation of volume fractions equals to one ($\xi_1 + \xi_2 = 1$). As seen from Eq. (4.1) choosing ξ_2 as zero gives classical constitutive relations and choosing ξ_1 as zero gives pure nonlocal constitutive relations in integral form. Here the kernel function can be chosen as a cone function, a bell function, and the Gaussian function or similar. By choosing the nonlocal kernel as a bi-exponential function the two-phase local-nonlocal shell constitutive relations can be written as given below for a well-known plane stress condition:

$$(4.3) \quad \begin{bmatrix} N_{zz}(z) \\ N_{ss}(z) \\ N_{sz}(z) \\ L_{zz}(z) \\ L_{ss}(z) \\ L_{sz}(z) \end{bmatrix} = \xi_1 \begin{bmatrix} A_{11} & A_{12} & A_{16} & B_{11} & B_{12} & B_{16} \\ & A_{22} & A_{26} & B_{12} & B_{22} & B_{26} \\ & & A_{66} & B_{16} & B_{26} & B_{66} \\ & & & D_{11} & D_{12} & D_{16} \\ & sym & & & D_{22} & D_{26} \\ & & & & & D_{66} \end{bmatrix} \begin{bmatrix} \varepsilon_{zz}^{(0)}(z) \\ \varepsilon_{ss}^{(0)}(z) \\ \gamma_{sz}^{(0)}(z) \\ \varepsilon_{zz}^{(1)}(z) \\ \varepsilon_{ss}^{(1)}(z) \\ \gamma_{sz}^{(1)}(z) \end{bmatrix} \\
 + \xi_2 \frac{1}{2\tau} \int e^{-\frac{|z-z'|}{\tau}} \begin{bmatrix} A_{11} & A_{12} & A_{16} & B_{11} & B_{12} & B_{16} \\ & A_{22} & A_{26} & B_{12} & B_{22} & B_{26} \\ & & A_{66} & B_{16} & B_{26} & B_{66} \\ & & & D_{11} & D_{12} & D_{16} \\ & sym & & & D_{22} & D_{26} \\ & & & & & D_{66} \end{bmatrix} \begin{bmatrix} \varepsilon_{zz}^{(0)}(z') \\ \varepsilon_{ss}^{(0)}(z') \\ \gamma_{sz}^{(0)}(z') \\ \varepsilon_{zz}^{(1)}(z') \\ \varepsilon_{ss}^{(1)}(z') \\ \gamma_{sz}^{(1)}(z') \end{bmatrix} dz'.$$

Here the nonlocal property is effective only in the z-direction. Assuming that the hoop stress resultant (N_{ss}) and the hoop stress couple (L_{ss}) are negligibly small. As the ξ_1 and ξ_2 are positive real numbers, in the equations of N_{ss} and L_{ss} both local and nonlocal part will be zero separately. This gives opportunity to extract $\varepsilon_{ss}^{(0)}$ and $\varepsilon_{ss}^{(1)}$ strains from the concerned equations. By substituting the extracted strains into Eq. (4.3) the modified constitutive relations can be defined in matrix form as presented below

$$(4.4) \quad \begin{bmatrix} N_{zz}(z) \\ N_{ss}(z) \\ N_{sz}(z) \\ L_{zz}(z) \end{bmatrix} = \xi_1 \begin{bmatrix} a_{11} & a_{16} & b_{11} & b_{16}^a \\ & a_{66} & b_{16}^b & B_{66} \\ & & d_{11} & d_{16} \\ & sym & & d_{66} \end{bmatrix} \begin{bmatrix} \varepsilon_{zz}^{(0)}(z) \\ \gamma_{sz}^{(0)}(z) \\ \varepsilon_{zz}^{(1)}(z) \\ \gamma_{sz}^{(1)}(z) \end{bmatrix} \\
 + \xi_2 \frac{1}{2\tau} \int e^{-\frac{|z-z'|}{\tau}} \begin{bmatrix} a_{11} & a_{16} & b_{11} & b_{16}^a \\ & a_{66} & b_{16}^a & b_{66} \\ & & d_{11} & d_{16} \\ & sym & & d_{66} \end{bmatrix} \begin{bmatrix} \varepsilon_{zz}^{(0)}(z') \\ \gamma_{sz}^{(0)}(z') \\ \varepsilon_{zz}^{(1)}(z') \\ \gamma_{sz}^{(1)}(z') \end{bmatrix} dz'.$$

Calculation of the elements of the modified constitutive relations can be found in detail in [29]. Here the non-zero elements for an isotropic material are expressed as following:

$$(4.5a) \quad a_{11} = Eh,$$

$$(4.5b) \quad a_{66} = Gh,$$

$$(4.5c) \quad d_{11} = E \frac{h^3}{12},$$

$$(4.5d) \quad d_{66} = G \frac{h^3}{12}.$$

The constitutive relations between the beam forces and the pole point displacements can be obtained by substituting the modified constitutive relations into Eqs. (3.5) as:

$$\begin{aligned}
 (4.6) \quad \begin{bmatrix} N_z(z) \\ M_y(z) \\ M_x(z) \\ M_\omega(z) \\ M_z(z) \end{bmatrix} &= \xi_1 \begin{bmatrix} e_{11} & e_{12} & e_{13} & e_{14} & e_{15} \\ & e_{22} & e_{23} & e_{24} & e_{25} \\ & & e_{33} & e_{34} & e_{35} \\ & & sym & e_{44} & e_{45} \\ & & & & e_{15} \end{bmatrix} \begin{bmatrix} W_0'(z) \\ -U''(z) \\ -V''(z) \\ -\phi''(z) \\ \phi'(z) \end{bmatrix} \\
 &+ \xi_2 \frac{1}{2\tau} \int e^{-\frac{|z-z'|}{\tau}} \begin{bmatrix} e_{11} & e_{12} & e_{13} & e_{14} & e_{15} \\ & e_{22} & e_{23} & e_{24} & e_{25} \\ & & e_{33} & e_{34} & e_{35} \\ & & sym & e_{44} & e_{45} \\ & & & & e_{15} \end{bmatrix} \begin{bmatrix} W_0'(z') \\ -U''(z') \\ -V''(z') \\ -\phi''(z') \\ \phi'(z') \end{bmatrix} dz',
 \end{aligned}$$

where $[e_{ij}]$ is called as the beam stiffness matrix. Elements of the beam stiffness matrix $[e_{ij}]$ is given in Appendix A.2.

5. Finite Element Method

The governing equations of the system is solved by the displacement based finite element method where the thin-walled beam is discretized with two node finite beam elements. Generalized displacements are expressed by using linear Lagrange ($S_{L,i}$) and hermetic-cubic ($S_{H,i}$) shape functions as:

$$(5.1a) \quad W = \sum_{i=1}^n w_i \cdot S_{L,i},$$

$$(5.1b) \quad U = \sum_{i=1}^n u_i \cdot S_{H,i},$$

$$(5.1c) \quad V = \sum_{i=1}^n v_i \cdot S_{H,i},$$

$$(5.1d) \quad \Phi = \sum_{i=1}^n \phi_i \cdot S_{H,i}.$$

Governing equations of the thin-walled beam having nonlocal property is expressed in the matrix form as given below by substituting Eq. (4.6) and Eqs. (5.1) into the weak formulation given in Eq. (3.7)

$$(5.2) \quad \left(\xi_1 \begin{bmatrix} K_{ij}^{11} & K_{ij}^{12} & K_{ij}^{13} & K_{ij}^{14} \\ & K_{ij}^{22} & K_{ij}^{23} & K_{ij}^{24} \\ & & K_{ij}^{33} & K_{ij}^{34} \\ sym & & & K_{ij}^{44} \end{bmatrix}^L + \xi_2 \begin{bmatrix} K_{ij}^{11} & K_{ij}^{12} & K_{ij}^{13} & K_{ij}^{14} \\ & K_{ij}^{22} & K_{ij}^{23} & K_{ij}^{24} \\ & & K_{ij}^{33} & K_{ij}^{34} \\ sym & & & K_{ij}^{44} \end{bmatrix}^{NL} \right) \begin{Bmatrix} w_i \\ i \\ v_i \\ \phi_i \end{Bmatrix}^\Delta = \begin{Bmatrix} fw_i \\ f \\ fv_i \\ f\phi_i \end{Bmatrix}^f.$$

Here $[K]^L$ and $[K]^{NL}$ are the local and nonlocal parts of the assembled global stiffness matrix, $\{\Delta\}$ is the displacement vector and $\{\mathbf{f}\}$ is the force vector. Displacements of the thin-walled beam having nonlocal property can be achieved by solving Eq. (5.2). Elements of the local stiffness matrix $[K]^L$ and the load vector $\{\mathbf{f}\}$ can be found in [30]. The elements of the nonlocal stiffness matrix $[K]^{NL}$ are given in reference [27] for the case of using the bi-exponential function as the nonlocal kernel.

6. Illustrative examples

In this section, the convergence of the developed finite element model is initially examined. Then validation of the presented model is realized by using available results and solutions in the literature. Finally, several loading cases are examined for nonlocal thin-walled beams. In the following calculations the beams shown in Fig. 2 are used. Dimensions and mechanical properties of the used beams are given in Table 1.

TABLE 1. Dimensions and mechanical properties of beams.

Beam Type	a	b	L	h	E	G	ν
Solid-Beam	1.667 [nm]	1.667 [nm]	20 [nm]	solid	68.5 [GPa]	26 [GPa]	0.32
Box-Beam	2 [μm]	1 [μm]	20 [μm]	0.1 [μm]	100 [GPa]	38.5 [GPa]	0.3
U-Beam	2 [μm]	1 [μm]	20 [μm]	0.1 [μm]	100 [GPa]	38.5 [GPa]	0.3

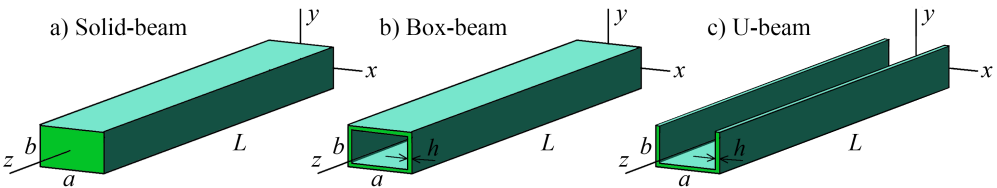


FIG. 2. Investigated beams having nonlocal property.

6.1. Convergence and validation

The convergence of the finite element solution is calculated by applying the simply supported boundary condition and the distributed load of $q_y = 1$ [N/m]

to the box-beam described above for the nonlocal parameter to the beam length ratio (τ/L) of 0.01, 0.1, 0.2 and the local volume fraction (ξ_1) of 0 (pure nonlocal case). As seen in Fig. 3 the finite element solution converges after 40 elements. The finite element solution of a nonlocal part needs much more elements than needed for a classical structure. Based on this convergence study, 50 finite beam elements are used to discretize the investigated thin-walled beams at all following calculations.

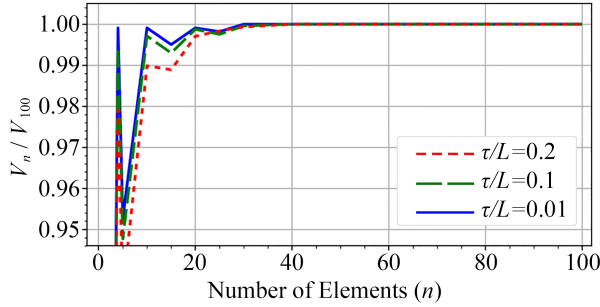


FIG. 3. Convergence of the finite element solution.

As explained in detail in Section 4, the presented model uses the integral formulation to define nonlocal constitutive relations. Because the developed model depends on the integral formulation, it is expected that the model could be used for any boundary condition and loading case, including the problematic cantilever beam problem. To further investigate the validity of the presented model, the acquired results have been compared with the results and solutions of FERNANDEZ *et al.* [22], CHALLAMEL *et al.* [21], and REDDY and PANG [31]. The closed form solutions of CHALLAMEL *et al.* [21] and REDDY and PANG [31] are summarized in Appendix A.3. During validation, the solid-beam defined in Table-1 has been used, the local volume fraction (ξ_1) has been set to zero and the nonlocal parameter to the beam length ratio (τ/L) has been varied from 0.005 up to 0.05 with steps of 0.005.

In the first validation case, simply supported nonlocal beams under a distributed load of 0.01 [N/m] are investigated. The maximum transverse deflection of the beams are calculated. The acquired results are compared with the solution of REDDY and PANG [31] and the results of FERNANDEZ [22] as presented in Fig. 4.

In the second validation case cantilever nonlocal beams under a concentrated tip load of 0.1 [nN] and under a distributed load of 0.01 [N/m] are investigated separately. Acquired results for the cantilever beams are compared with the solution of CHALLAMEL *et al.* [21] and the results of FERNANDEZ [22] as given in Figs. 5 and 6.

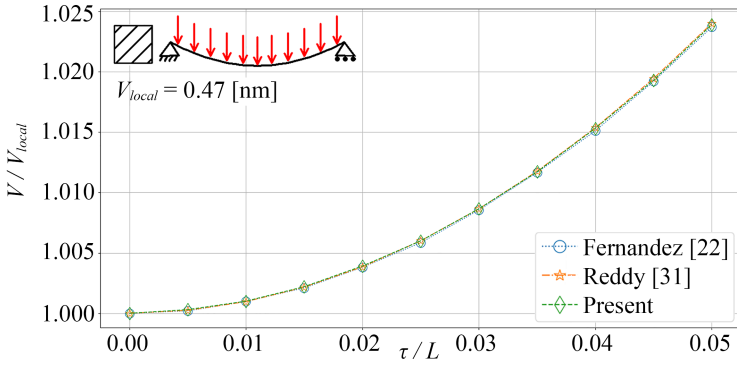


FIG. 4. Normalized transverse deflection for simply supported nonlocal solid-beam under distributed load $q_y = 0.01$ [N/m].

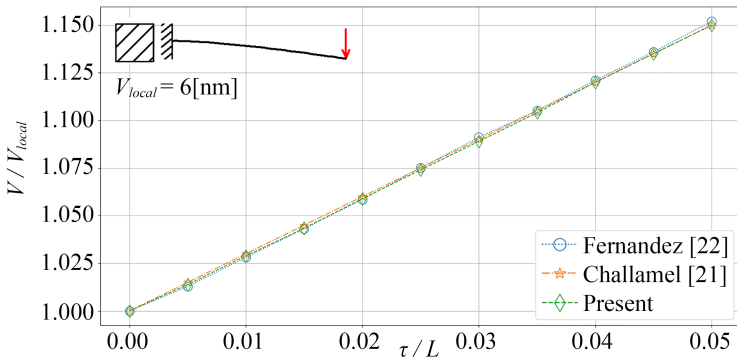


FIG. 5. Normalized transverse deflection for cantilever nonlocal solid-beam under concentrated load $F_y = 0.1$ [nN].

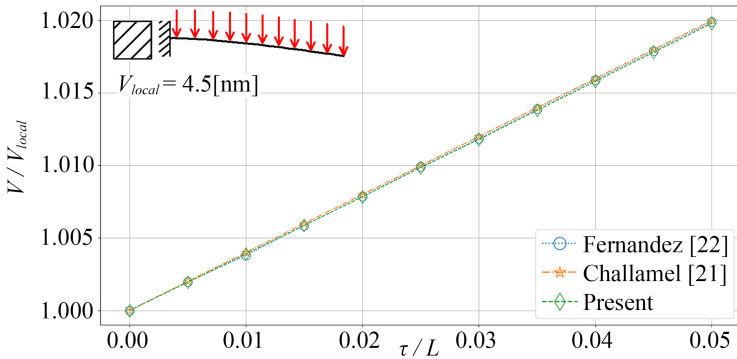


FIG. 6. Normalized transverse deflection for cantilever nonlocal solid-beam under distributed load $q_y = 0.01$ [N/m].

As seen in Figs. 4–6 the results of the developed model are perfectly in alignment with the results of FERNANDEZ *et al.* [22] and also with solutions of CHALLAMEL *et al.* [21] and REDDY and PANG [31]. It is seen that, the integral formulation does not show ill-posed properties as differential formulation shows. This finding has been also mentioned by CHALLAMEL *et al.* [21] and FERNANDEZ *et al.* [22].

6.2. Distributed load case for thin-walled beams

In this section simply supported, clamped-clamped and clamped-free (cantilever) thin-walled box-beams and U-beams, which are defined in Table 1, are investigated for various τ/L ratios and ξ_1 volume fraction values. In calculations, the volume fraction of local phase (ξ_1) is increased from 0 to 1 with steps of 0.01 and the τ/L ratio is increased from 0.01 up to 0.25 with steps of 0.02. A distributed load of $q_y = 0.001$ [N/m] is applied to micro-scale thin-walled box-beams and U-beams. Maximum transverse deflection results of box-beams are presented in Fig. 7 for simply supported, clamped-clamped and clamped-free boundary conditions, respectively. Similarly, maximum transverse deflections of U-beams are given in Fig. 8.

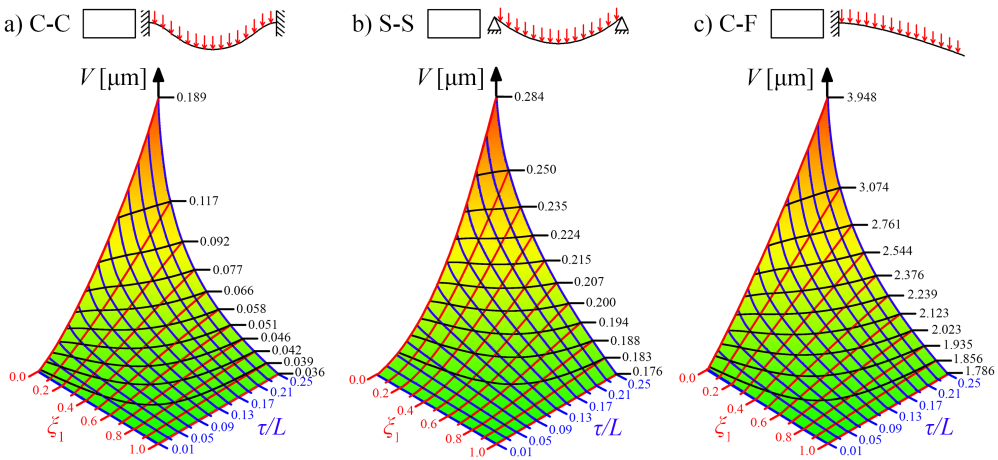


FIG. 7. Transverse deflection of box-beams under distributed load $q_y = 0.001$ [N/m].

When Fig. 7 is investigated it is observed that increasing the τ/L ratio or decreasing the ξ_1 local phase volume fraction reduces the bending rigidity of the beams thus the deflection increases. This situation is valid for all boundary conditions. In Fig. 7 blue lines represent the relation between the deflection and the ξ_1 volume fraction for a specific τ/L ratio. And inversely, red lines represent

the relation between the deflection and the τ/L ratio for a specific ξ_1 value. As obviously seen in Fig. 7a and Fig. 7b blue and red lines have a nonlinear character for simply supported and clamped-clamped beams. This means that for simply supported and clamped-clamped boundary conditions the nonlocal τ/L and ξ_1 parameters affect the beams nonlinearly. On the other hand, red lines look almost linear for the clamped-free beams as seen in Fig. 7c. Besides the red and blue lines, the black lines represent the iso-curves of the transverse deflection. These iso-curves indicate that the same deflection value can be obtained by various combinations of τ/L and ξ_1 parameters.

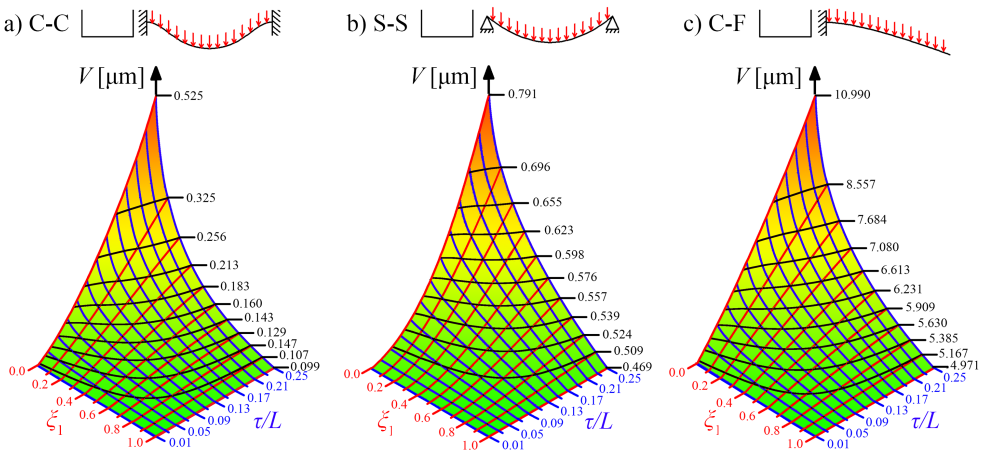


FIG. 8. Transverse deflection of U beams under distributed load $q_y = 0.001$ [N/m].

When the deflection of box-beams having a closed cross-section and the deflection of U beams having an open cross-section are compared, it is visible that the box-beams and U -beams show almost the same characteristics for the same boundary conditions and parameters. The main difference between them is the value of the deflection. This situation is reasonable as the nonlocal property is only applied along the beam length and it does not affect the cross-section of the beams in the current model.

In order to compare the effect of the nonlocal parameters on the beams with different boundary conditions the deflection values of $\xi_1 = 0$, $\xi_1 = 0.33$, $\xi_1 = 0.66$ and $\xi_1 = 1$ cases have been normalized by dividing them by their local ($\xi_1 = 1$) values. The normalized values are presented in Table 2, respectively for clamped-clamped, clamped-free and simply supported boundary conditions.

TABLE 2. Normalized values for each boundary condition ($\hat{V} = V/V_{\xi_1=1}$).

		Box-Beam				U-Beam			
C-C	τ/L	$\xi_1 = 0$	$\xi_1 = 0.33$	$\xi_1 = 0.66$	$\xi_1 = 1$	$\xi_1 = 0$	$\xi_1 = 0.33$	$\xi_1 = 0.66$	$\xi_1 = 1$
	0.05	1.44	1.20	1.08	1	1.44	1.20	1.08	1
hline	0.1	2.10	1.43	1.17	1	2.10	1.43	1.17	1
	0.15	2.93	1.67	1.26	1	2.93	1.67	1.26	1
	0.2	3.99	1.90	1.32	1	3.99	1.90	1.32	1
	0.25	5.29	2.11	1.37	1	5.29	2.11	1.37	1
C-F	τ/L	$\xi_1 = 0$	$\xi_1 = 0.33$	$\xi_1 = 0.66$	$\xi_1 = 1$	$\xi_1 = 0$	$\xi_1 = 0.33$	$\xi_1 = 0.66$	$\xi_1 = 1$
	0.05	1.19	1.09	1.04	1	1.19	1.09	1.04	1
	0.1	1.42	1.17	1.07	1	1.42	1.17	1.07	1
	0.15	1.66	1.25	1.10	1	1.66	1.25	1.10	1
	0.2	1.92	1.33	1.13	1	1.92	1.33	1.13	1
	0.25	2.21	1.41	1.16	1	2.21	1.41	1.16	1
S-S	τ/L	$\xi_1 = 0$	$\xi_1 = 0.33$	$\xi_1 = 0.66$	$\xi_1 = 1$	$\xi_1 = 0$	$\xi_1 = 0.33$	$\xi_1 = 0.66$	$\xi_1 = 1$
	0.05	1.02	1.01	1.01	1	1.02	1.01	1.01	1
	0.1	1.10	1.05	1.03	1	1.10	1.05	1.03	1
	0.15	1.21	1.11	1.05	1	1.21	1.11	1.05	1
	0.2	1.38	1.18	1.08	1	1.38	1.18	1.08	1
	0.25	1.60	1.25	1.10	1	1.60	1.25	1.10	1

When the normalized values are inspected in Table 2 it can be inferred that using the same τ/L ratio and ξ_1 volume fraction affect the simply supported beams least (1.6 for $\xi_1 = 0$ and $\tau/L = 0.25$) and clamped-clamped beams most (5.29 for $\xi_1 = 0$ and $\tau/L = 0.25$). The clamped-free beams lay between them (2.21 for $\xi_1 = 0$ and $\tau/L = 0.25$). No difference is observed between the normalized deflection values of box-beams and U-beams as the nonlocal parameters are only effective along the beam length in the presented model.

6.3. Torsional load case for thin-walled beams

The torsional analysis of clamped-free box-beams and U-beams have been realized by applying a torsional moment of $0.1 [\mu\text{N} \cdot \mu\text{m}]$ to the free tip of beams. Surface plots of the axial rotation of the free tip with respect to τ/L and ξ_1 values are given in Fig. 9 for box-beams and U-beams.

As seen in Fig. 9 the axial rotation increases as the τ/L ratio gets increased or ξ_1 volume fraction gets decreased. In the surface plots given above blue lines (relation between Φ and ξ_1) are nonlinear, on the other hand red lines (relation

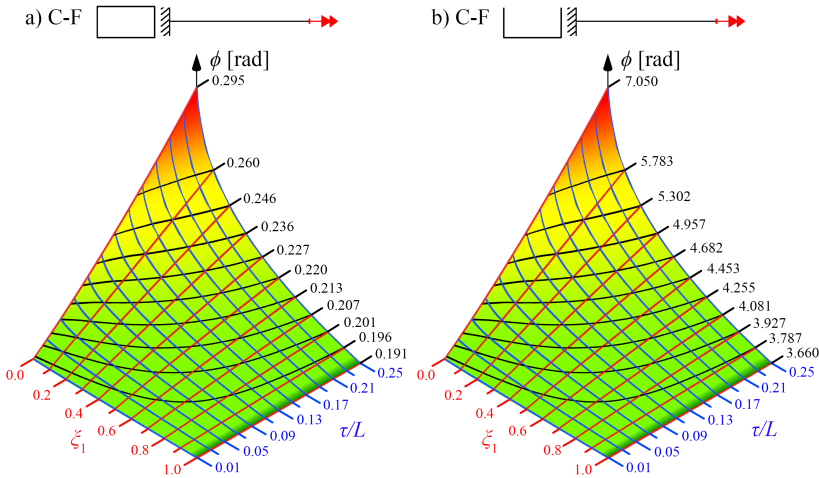


FIG. 9. Axial rotation of the free tip for (a) box-beams and (b) U-beams $M_z = 0.1 [\mu\text{N} \cdot \mu\text{m}]$.

between Φ and τ/L) is almost linear. Again, black lines represent the iso-curves of the deformation which can be acquired by using various combinations of τ/L and ξ_1 parameters.

At the free tip of the beams the warping deformation occurs as a result of torsional loads or torsion coupled deformations. Primary warping profiles of the cross-sections are given in Fig. 10 for box-beams and U-beams. During primary warping deformation, the corners of the cross-section displace inward and outward equally. But here it should be noted that the open corners of the U cross-section will have zero warping displacement.

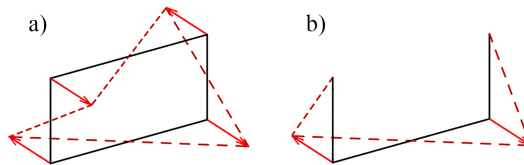


FIG. 10. Warping profiles for (a) box-beam and (b) U-beam.

The primary warping displacements of the corners of the beams are calculated using Eq. (2.1c) for the torsional load case described above and they are presented in Table 3 for box-beams and in Table 4 for U-beams. Here similar to the axial rotation, the warping displacements of the cross-section increase as the τ/L ratio increases or ξ_1 volume fraction decreases.

TABLE 3. Warping displacement of corners for box-beam.

τ/L	Nonlocal	W_{warp} [nm]									Local
	$\xi_1 = 0$	0.1	0.2	0.3	0.4	0.5	0.6	0.7	0.8	0.9	$\xi_1 = 1$
0.01	1.65	1.64	1.62	1.61	1.60	1.59	1.58	1.58	1.57	1.56	1.55
0.03	1.90	1.84	1.79	1.75	1.72	1.68	1.65	1.62	1.60	1.57	1.55
0.05	2.18	2.05	1.96	1.88	1.82	1.76	1.71	1.66	1.62	1.59	1.55
0.07	2.47	2.26	2.11	2.00	1.90	1.82	1.76	1.70	1.64	1.59	1.55
0.09	2.76	2.45	2.24	2.09	1.97	1.87	1.79	1.72	1.65	1.60	1.55
0.11	3.06	2.62	2.35	2.17	2.02	1.91	1.81	1.73	1.66	1.60	1.55
0.13	3.37	2.77	2.45	2.23	2.07	1.94	1.84	1.75	1.67	1.61	1.55
0.15	3.67	2.91	2.53	2.28	2.10	1.96	1.85	1.76	1.68	1.61	1.55
0.17	3.98	3.04	2.60	2.33	2.13	1.98	1.87	1.77	1.69	1.61	1.55
0.19	4.29	3.15	2.66	2.37	2.16	2.00	1.88	1.78	1.69	1.62	1.55
0.21	4.61	3.25	2.72	2.40	2.18	2.02	1.89	1.78	1.69	1.62	1.55
0.23	4.93	3.34	2.76	2.43	2.20	2.03	1.90	1.79	1.70	1.62	1.55
0.25	5.25	3.42	2.81	2.45	2.22	2.04	1.91	1.79	1.70	1.62	1.55

TABLE 4. Warping displacement of corners for U-beam.

τ/L	Nonlocal	W_{warp} [nm]									Local
	$\xi_1 = 0$	0.1	0.2	0.3	0.4	0.5	0.6	0.7	0.8	0.9	$\xi_1 = 1$
0.01	6.74	6.70	6.65	6.61	6.57	6.53	6.49	6.49	6.45	6.42	6.41
0.03	7.74	7.52	7.33	7.17	7.02	6.89	6.77	6.77	6.65	6.55	6.41
0.05	8.87	8.37	8.01	7.71	7.44	7.21	7.00	7.00	6.82	6.65	6.41
0.07	10.04	9.21	8.62	8.16	7.78	7.46	7.18	7.18	6.94	6.72	6.41
0.09	11.25	9.98	9.16	8.54	8.05	7.66	7.32	7.32	7.03	6.77	6.41
0.11	12.47	10.69	9.61	8.85	8.27	7.81	7.42	7.42	7.10	6.82	6.41
0.13	13.71	11.32	10.00	9.11	8.45	7.93	7.51	7.51	7.15	6.85	6.41
0.15	14.96	11.88	10.34	9.33	8.60	8.03	7.58	7.58	7.20	6.88	6.41
0.17	16.21	12.39	10.62	9.51	8.72	8.12	7.64	7.64	7.23	6.90	6.41
0.19	17.49	12.85	10.87	9.67	8.83	8.19	7.68	7.68	7.27	6.92	6.41
0.21	18.78	13.26	11.09	9.81	8.92	8.25	7.73	7.73	7.30	6.93	6.41
0.23	20.08	13.62	11.29	9.93	9.00	8.31	7.77	7.77	7.32	6.95	6.41
0.25	21.40	13.96	11.46	10.03	9.07	8.36	7.80	7.80	7.35	6.96	6.41

6.4. Concentrated load case for thin-walled cantilever beams

In this example, a concentrated load of $0.01 [\mu\text{N}]$ has been applied to the free end of the cantilever box-beams and U-beams. In calculations, the volume fraction of the local phase (ξ_1) is increased from 0 to 1 with steps of 0.01 and the τ/L ratio is increased from 0.025 up to 0.25 with steps of 0.025. Surface plots

of the transverse deflection of the free tip with respect to τ/L and ξ_1 values are given in Fig. 11 for box-beams and U beams. As seen in Fig. 11 the developed model is capable of solving the cantilever beam problem. It is seen that, reducing the local volume fraction (ξ_1) or increasing the nonlocal parameter (τ/L) softens the beam stiffness as expected and the deflection increases with this softening.

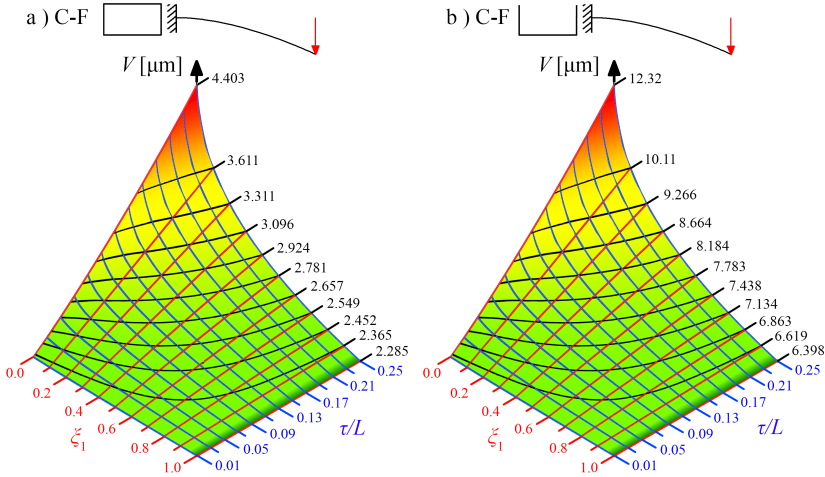


FIG. 11. Transverse deflection of the free tip for (a) box and (b) U-beams, $F_y = 0.01 \text{ [}\mu\text{N]}$.

Additional to transverse deflection, U-beams shows coupled displacement and rotation because of their open cross-section. As an example, for the cantilever beam given in Fig. 11b the coupled displacement and rotation values are given

TABLE 5. Coupled displacement of free and for cantilever U-beam.

τ/L	Nonlocal	$U \text{ [}\mu\text{m]}$									Local
	$\xi_1 = 0$	0.1	0.2	0.3	0.4	0.5	0.6	0.7	0.8	0.9	$\xi_1 = 1$
0.025	0.076	0.075	0.075	0.074	0.074	0.073	0.073	0.072	0.072	0.072	0.071
0.050	0.082	0.079	0.078	0.076	0.075	0.075	0.074	0.073	0.073	0.072	0.071
0.075	0.088	0.083	0.081	0.079	0.077	0.076	0.075	0.074	0.073	0.072	0.071
0.100	0.094	0.087	0.084	0.081	0.079	0.078	0.076	0.075	0.074	0.073	0.071
0.125	0.101	0.091	0.087	0.084	0.081	0.079	0.077	0.076	0.074	0.073	0.071
0.150	0.107	0.095	0.090	0.086	0.083	0.081	0.079	0.077	0.075	0.073	0.071
0.175	0.114	0.099	0.093	0.089	0.085	0.082	0.080	0.077	0.075	0.073	0.071
0.200	0.121	0.103	0.096	0.091	0.087	0.084	0.081	0.078	0.076	0.074	0.071
0.225	0.129	0.107	0.099	0.093	0.089	0.085	0.082	0.079	0.077	0.075	0.071
0.250	0.135	0.111	0.102	0.096	0.091	0.086	0.083	0.080	0.077	0.075	0.071

TABLE 6. Coupled axial rotation of free and for cantilever U-beam.

τ/L	Nonlocal	ϕ [rad]									Local
	$\xi_1 = 0$	0.1	0.2	0.3	0.4	0.5	0.6	0.7	0.8	0.9	$\xi_1 = 1$
0.025	0.126	0.124	0.123	0.122	0.121	0.121	0.120	0.120	0.119	0.119	0.117
0.050	0.136	0.130	0.128	0.126	0.125	0.123	0.122	0.121	0.120	0.119	0.117
0.075	0.146	0.137	0.133	0.130	0.128	0.126	0.124	0.122	0.121	0.119	0.117
0.100	0.156	0.143	0.138	0.134	0.131	0.128	0.126	0.124	0.122	0.120	0.117
0.125	0.166	0.150	0.143	0.138	0.134	0.131	0.128	0.125	0.123	0.120	0.117
0.150	0.177	0.156	0.148	0.142	0.137	0.133	0.130	0.126	0.124	0.121	0.117
0.175	0.188	0.163	0.153	0.146	0.141	0.136	0.131	0.128	0.124	0.121	0.117
0.200	0.200	0.170	0.158	0.150	0.144	0.138	0.133	0.129	0.125	0.122	0.117
0.225	0.213	0.177	0.164	0.154	0.147	0.140	0.135	0.130	0.126	0.123	0.117
0.250	0.223	0.184	0.169	0.158	0.150	0.143	0.137	0.131	0.127	0.124	0.117

in Table 5 and Table 6. As seen in the following tables, the coupled displacements and rotations behaves similar to primary displacement for same nonlocal parameters.

7. Conclusion

The main goal of this work is to develop a model for static analysis of small-scale thin-walled beams showing nonlocal property. The developed model is obtained by implementing integral formulation of local-nonlocal two-phase constitutive relations into thin-walled beams theory. The developed model includes flexural-torsional coupling, warping effects and as well as nonlocal elasticity. Solution of the model is realized by the displacement based finite element method. The performed validations show that the developed model is compatible with the results and solutions available in the literature. Additionally, the developed model is able solve nonlocal cantilever beams under concentrated tip load. This is possible because of the constitutive relations are directly modelled using the integral formulation of the nonlocal elasticity theory. Another advantage of using the integral formulation is that it gives opportunity to change the nonlocal kernel function of the model easily.

As numerical examples, effects of the volume fraction and the nonlocal parameter on the deformation of the small-scale box-beams and U-beams are investigated for various conditions. The following findings are observed.

- The stiffness of the beam reduces as the τ/L ratio gets increased or the ξ_1 local phase volume fraction gets decreased.
- The relation between the deformation and nonlocal parameters τ/L and ξ_1 usually shows a nonlinear character for investigated boundary conditions.

But for clamped-free beams the relation between τ/L and deformation looks linear both for transverse deflection and axial rotation cases.

- When boundary conditions are compared it is observed that the clamped-clamped beams get affected most and the simply supported beams least by the non-local parameters.
- For beams showing flexural-torsional coupling, the coupled displacements and rotations get affected by the nonlocal parameters similar to primary displacement.
- The warping of the cross-section gets affected by nonlocal parameters, depended on the axial rotation or flexural-torsional coupling.
- As the developed model includes two independent parameters (τ and ξ), the same displacement value can be obtained by various combinations of these parameters.
- Thanks to integral formulation the developed model is able to solve non-local cantilever beams under a concentrated tip load.

The presented model in this study can be enhanced by including shear deformation, cross-sectional deformation and nonlinear formulation. Other size depended theories such as the strain gradient theory, the micro-polar theory may be implemented in the model. Also, nonlocality can be applied along the cross-section together with cross-sectional deformation.

Appendix

A.1. Definitions of the $r_s(s)$, $r_n(s)$ distances and the warping functions

$$(A.1a) \quad r_s(s) = (x(s) - x_p) \frac{dx}{ds} + (y(s) - y_p) \frac{dy}{ds},$$

$$(A.1b) \quad r_n(s) = (x(s) - x_p) \frac{dy}{ds} - (y(s) - y_p) \frac{dx}{ds},$$

$$(A.1c) \quad \mathcal{F}_1(s) = \int_0^s (r_n(s)) ds - \delta_c \int_0^s \left(\frac{\oint r_n(s) ds}{h(s) \cdot G_{sz}(s) \cdot L} \right) ds,$$

$$(A.1d) \quad \mathcal{F}_2(s) = \delta_c \int_0^s \left(2 - \frac{2 \oint ds}{h(s) \cdot G_{sz}(s) \cdot L} \right) ds - r_s(s),$$

$$(A.1e) \quad \mathcal{L} = \oint \frac{ds}{h(s) \cdot G_{sz}(s)},$$

where h is the thickness and G_{sz} is the effective shear stiffness. Take $\delta_0 = 1$, $\delta_c = 0$ for open cross-sections or $\delta_0 = 0$, $\delta_c = 1$ for closed cross-sections.

A.2. Elements of the $[e_{ij}]$ beam stiffness matrix

$$(A.2a) \quad e_{11} = \int_s a_{11} ds,$$

$$(A.2b) \quad e_{12} = \int_s a_{11}(s) ds,$$

$$(A.2c) \quad e_{13} = \int_s a_{11}y(s) ds,$$

$$(A.2d) \quad e_{14} = \int_s a_{11}\mathcal{F}_1(s) ds,$$

$$(A.2e) \quad e_{22} = \int_s \left(a_{11}x(s)^2 + d_{11} \left(\frac{dy}{ds} \right)^2 \right) ds,$$

$$(A.2f) \quad e_{23} = \int_s \left(a_{11}x(s)y(s) - d_{11} \frac{dx}{ds} \frac{dy}{ds} \right) ds,$$

$$(A.2g) \quad e_{24} = \int_s \left(a_{11}x(s)\mathcal{F}_1(s) + d_{11}\mathcal{F}_2(s) \frac{dy}{ds} \right) ds,$$

$$(A.2h) \quad e_{33} = \int_s \left(a_{11}y(s)^2 + d_{11} \left(\frac{dx}{ds} \right)^2 \right) ds,$$

$$(A.2i) \quad e_{34} = \int_s \left(a_{11}y(s)\mathcal{F}_1(s) - d_{11}\mathcal{F}_2(s) \frac{dx}{ds} \right) ds,$$

$$(A.2j) \quad e_{44} = \int_s \left(a_{11}\mathcal{F}_1(s)^2 + d_{11}\mathcal{F}_2(s)^2 \right) ds,$$

$$(A.2k) \quad e_{55} = \int_s \left(a_{66} \left(\delta_c \frac{2\Omega}{h(s)G_{sz}(s)\mathcal{L}} \right)^2 + d_{66} \left(\delta_c \frac{2\beta}{h(s)G_{sz}(s)\mathcal{L}} + \delta_0 2 \right)^2 \right) ds.$$

A.3. The closed form solutions**A.3.1. Tip deflection of cantilever beam under concentrated transverse end load [21]**

$$(A.3a) \quad w(L) = P \frac{L^3}{3EI} \left(1 + \frac{3l_c}{L^2} \right).$$

A.3.2. Mid deflection of simply supported beam under distributed transverse load [31]

$$(A.3b) \quad w\left(\frac{L}{2}\right) = q_0 \frac{L^4}{384EI} (5 + 48 \cdot \bar{\mu}), \quad \bar{\mu} = \left(\frac{e_0 \cdot l_i}{L} \right)^2.$$

Acknowledgements

The numerical calculations reported in this paper were partially performed at TUBITAK ULAKBIM, High Performance and Grid Computing Center (TRUBA resources). No other support from any organization for the submitted work is received.

Conflict of interest

The author certifies that he has no affiliations or involvement with any organization or entity nor does he have a financial interest or non-financial interest in the subject matter or materials discussed in this manuscript.

References

1. S.P. TIMOSHENKO, J.N. GOODIER, *Theory of Elasticity*, McGraw-Hill, New York, 1951.
2. V.Z. VLASOV, *Thin-Walled Elastic Beams*, National Technical Information Service, Washington DC, 1961.
3. A. GJELSVIK, *The Theory of Thin-Walled Bars*, Wiley, New York, 1981.
4. L.S. LIBRESCU, *Thin-walled Composite Beams: Theory and Application*, Springer, Netherlands, 2005.
5. A.C. ERINGEN, *Theory of nonlocal elasticity and some applications*, Res Mechanica, **21**, 4, 313–342, 1987.
6. N.A. FLECK, J.W. HUTCHINSON, *A phenomenological theory for strain gradient effects in plasticity*, Journal of the Mechanics and Physics of Solids, **41**, 12, 1825–1857, 1993.
7. H. NEUBER, *On the general solution of linear-elastic problems in isotropic and anisotropic Cosserat continua*, in: *Applied Mechanics*, pp. 153–158, Springer, Berlin, 1966.
8. M.E. GURTIN, A.I. MURDOCH, *Surface stress in solids*, International Journal of Solids and Structures, **14**, 6, 431–440, 1978.
9. J. PEDDIENSON, G.R. BUCHANAN, R.P. MCNITT, *Application of nonlocal continuum models to nanotechnology*, International Journal of Engineering Science, **41**, 3-5, 305–312, 2003.
10. N. CHALLAMEL, C. WANG, *The small length scale effect for a non-local cantilever beam: a paradox solved*, Nanotechnology, **19**, 34, 345703, 2008.
11. G. ROMANO, R. BARRETTA, M. DIACO, F.M. DE SCIARRA, *Constitutive boundary conditions and paradoxes in nonlocal elastic nanobeams*, International Journal of Mechanical Sciences, **121**, 151–156, 2017.
12. C. LI, L.Q. YAO, W.Q. CHEN, S. LI, *Comments on nonlocal effects in nano-cantilever beams*, International Journal of Engineering Science, **87**, 47–57, 2015.
13. R. BARRETTA, F.M. DE SCIARRA, *Constitutive boundary conditions for nonlocal strain gradient elastic nano-beams*, International Journal of Engineering Science, **130**, 187–198, 2018.
14. C. POLIZZOTTO, *Nonlocal elasticity and related variational principles*, International Journal of Solids and Structures, **38**, 42–43, 7359–7380, 2001.
15. N. CHALLAMEL, C. WANG, I. ELISHAKOFF, *Discrete systems behave as nonlocal structural elements: bending, buckling and vibration analysis*, European Journal of Mechanics-A/Solids, **44**, 125–135, 2014.

16. M.F. OSKOUIE, R. ANSARI, H. ROUHI, *Bending of Euler–Bernoulli nanobeams based on the strain-driven and stress-driven nonlocal integral models: a numerical approach*, Acta Mechanica Sinica, **34**, 871–882, 2018.
17. G. ROMANO, R. BARRETTA, *Nonlocal elasticity in nanobeams: the stress-driven integral model*, International Journal of Engineering Science, **115**, 14–27, 2017.
18. F.P. PINNOLA, M.S. VACCARO, R. BARRETTA, F.M. DE SCIARRA, *Random vibrations of stress-driven nonlocal beams with external damping*, Meccanica, **56**, 1329–1344, 2021.
19. F.P. PINNOLA, M.S. VACCARO, R. BARRETTA, F.M. DE SCIARRA, *Finite element method for stress-driven nonlocal beams*, Engineering Analysis with Boundary Elements, **134**, 22–34, 2022.
20. A.A. PISANO, P. FUSCHI, C. POLIZZOTTO, *Integral and differential approaches to Eringen’s nonlocal elasticity models accounting for boundary effects with applications to beams in bending*, ZAMM-Journal of Applied Mathematics and Mechanics (Zeitschrift für Angewandte Mathematik und Mechanik), **101**, 8, 202000152, 2021.
21. N. CHALLAMEL, J. REDDY, C. WANG, *Eringen’s stress gradient model for bending of nonlocal beams*, Journal of Engineering Mechanics, **142**, 12, 04016095, 2016.
22. J. FERNANDEZ-SAEZ, R. ZAERA, J.A. LOYA, J.N. REDDY, *Bending of Euler–Bernoulli beams using Eringen’s integral formulation: a paradox resolved*, International Journal of Engineering Science, **99**, 107–116, 2016.
23. A.D. POLYANIN, A.V. MANZHIROV, *Handbook of Integral Equations*, CRC Press, New York, 2008.
24. H.C. LI, L.L. KE, J. YANG, S. KITIPORNCHAI, *Size-dependent free vibration of microbeams submerged in fluid*, International Journal of Structural Stability and Dynamics, **20**, 12, 2020.
25. M. GHANE, A.R. SAIDI, R. BAHAADINI, *Vibration of fluid-conveying nanotubes subjected to magnetic field based on the thin-walled Timoshenko beam theory*, Applied Mathematical Modelling, **80**, 65–83, 2020.
26. M. SOLTANI, F. ATOUFI, F. MOHRI, R. DIMITRI, *Nonlocal elasticity theory for lateral stability analysis of tapered thin-walled nanobeams with axially varying materials*, Thin-Walled Structures, **159**, 2021.
27. M.G. GÜNAY, *Buckling analysis of thin-walled beams by two-phase local–nonlocal integral model*, Iranian Journal of Science and Technology, Transactions of Mechanical Engineering, **47**, 2, 765–777, 2023.
28. M.G. GÜNAY, *Free vibration analysis of thin-walled beams using two-phase local–nonlocal constitutive model*, Journal of Vibration and Acoustics, **145**, 3, 031009, 2023.
29. M.G. GÜNAY, T. TIMARCI, *Stresses in thin-walled composite laminated box-beams with curvilinear fibers: Antisymmetric and symmetric fiber paths*, Thin-Walled Structures, **138**, 170–182, 2019.
30. M.G. GÜNAY, T. TIMARCI, *Static analysis of thin-walled laminated composite closed-section beams with variable stiffness*, Composite Structures, **182**, 67–78, 2017.
31. J. REDDY, S. PANG, *Nonlocal continuum theories of beams for the analysis of carbon nanotubes*, Journal of Applied Physics, **103**, 2, 023511, 2008.

Received August 8, 2023; revised version October 21, 2023.

Published online November 29, 2023.